

$D^{*\pm}$ Meson Production in Deep Inelastic Scattering and Photoproduction with the H1 Detector at HERA

Andreas Werner Jung for the H1 collaboration

University of Heidelberg - Kirchhoff-Institute for Physics
Im Neuenheimer Feld 227, 69120 Heidelberg - Germany

Preliminary results on inclusive production of $D^{*\pm}$ mesons in photoproduction (γ P) and deep inelastic scattering (DIS) using the H1 detector at HERA are presented. The cross section measurements are compared to NLO calculations using the DGLAP evolution and LO Monte Carlo predictions based on the DGLAP and CCFM evolution scheme.

1 Introduction

The charm quark production in ep scattering is dominated by the boson-gluon-fusion (BGF) process. For the presented analyses [1] the kinematic range is divided into two regions of the photon virtuality Q^2 : The DIS regime covers $Q^2 > 5 \text{ GeV}^2$ while $Q^2 \approx 0$ is called the photoproduction regime. Due to the presence of many hard scales (m_c, Q^2, p_T) the predictive power of perturbative QCD (pQCD) is decreased since the choice of a hard scale is no longer unique. If one of the other scales is much larger than the mass, massless schemes where the mass of the produced quark is neglected can be applied otherwise massive schemes are applied. Because of the dominant BGF production process the charm cross section is directly sensitive to the gluon density in the proton.

2 Data samples

In both kinematic regions charm events are tagged by $D^{*\pm}$ mesons reconstructed in the golden decay channel: $D^{*\pm} \rightarrow D^0 \pi_{\text{slow}}^\pm \rightarrow K^\mp \pi^\pm \pi_{\text{slow}}^\pm$. The phase space and the luminosity

used for the two analyses is summarized in Table 1. The visible range is defined by Q^2 , the inelasticity y and by the kinematic quantities of the $D^{*\pm}$ meson: the transverse momentum p_T and the pseudorapidity η . For completeness also the range of the energy in the photon proton rest frame called $W_{\gamma P}$ is given. The significantly increased kinematic range compared to the previous tagged electron analysis [2] for the photoproduction regime was made possible

| | DIS | γ P |
|----------------------|-------------------------------|------------------------------|
| Luminosity | 348 pb^{-1} | 93 pb^{-1} |
| Q^2 | $5 < Q^2 < 100 \text{ GeV}^2$ | $Q^2 < 2 \text{ GeV}^2$ |
| y | $0.02 < y < 0.70$ | $0.10 < y < 0.80$ |
| $W_{\gamma P}$ [GeV] | $45 < W_{\gamma P} < 265$ | $100 < W_{\gamma P} < 285$ |
| $p_T(D^{*\pm})$ | $p_T(D^*) > 1.5 \text{ GeV}$ | $p_T(D^*) > 1.8 \text{ GeV}$ |
| $\eta(D^{*\pm})$ | $ \eta(D^*) < 1.5$ | $ \eta(D^*) < 1.5$ |

Table 1: The table summarizes the luminosity and the visible kinematic range per analysis.

by the use of the H1 Fast Track Trigger (FTT) [3, 4] where especially the rate reduction capabilities of the FTT Level Three [5] allowed the collection of an untagged electron sample where the electron remains undetected. The DIS analysis uses electron and hadron quantities combined in the $e\Sigma$ reconstruction method [6] for the reconstruction of the kinematic

variables which allows lower y and smaller systematic uncertainties compared to previous DIS analyses [7].

3 Theoretical models

The photoproduction cross section measurement is compared to the LO MC predictions from PYTHIA [8] based on the DGLAP evolution scheme. In the γP regime resolved processes, where the photon fluctuates into a hadronic system, have to be taken into account. Therefore PYTHIA is used in two different modes since it simulates the direct process either in a massless or a massive calculation. The resolved process is always treated massless. In addition, CASCADE [9] based on the CCFM evolution involving the k_T -unintegrated gluon distribution in the proton is used for comparisons. In addition, the massive NLO calculation from FMNR [10] in the fixed flavor number scheme (FFNS) is used for comparison where the dominant theoretical error arises from the scale uncertainty.

The DIS cross sections are compared to the massive NLO calculation HVQDIS [11] in the FFNS. Two different proton parton density functions (PDF), namely CTEQ5f3 [12] and MRST04FF3nlo [13], have been used with HVQDIS. The dominant theoretical error on HVQDIS arises from the charm mass uncertainty. In the DIS region contributions from resolved processes are found to be negligible. The LO MC programs RAPGAP [14], based on the DGLAP evolution scheme, with two different proton PDFs and CASCADE are also used for comparisons.

4 Cross section measurement

The $D^{*\pm}$ cross section measurement figures are organized such that the DIS regime (left) and the γP regime (right) are shown in the same figure. It should be mentioned that the

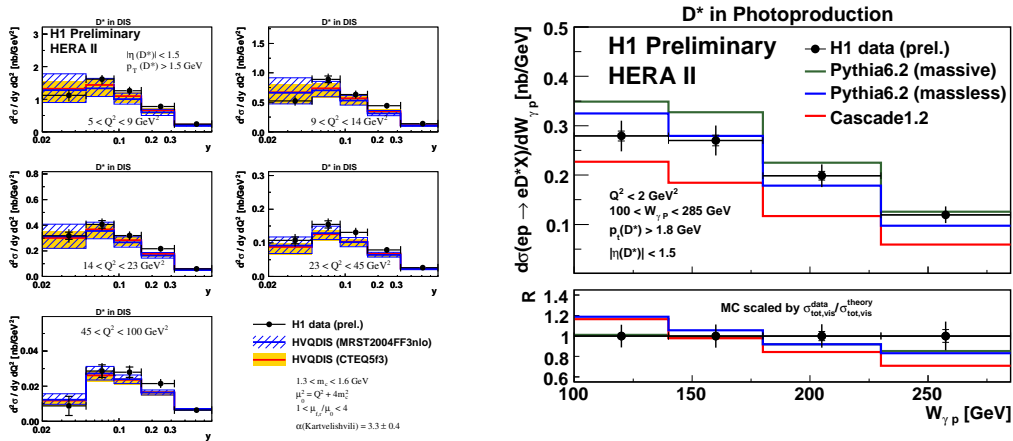


Figure 1: The double differential cross section in y and Q^2 is shown for the DIS (left) whereas for the photoproduction (right) regime the cross section as a function of $W_{\gamma P}$ is shown. The lower plot shows the ratio $R = \text{data}/\text{MC}$ as described in the text.

normalisation of LO MC predictions are not expected to fit. In order to better judge on the shapes the ratio between data and the predictions normalised to the respective total visible cross section is shown at the bottom of a single differential distribution. For the

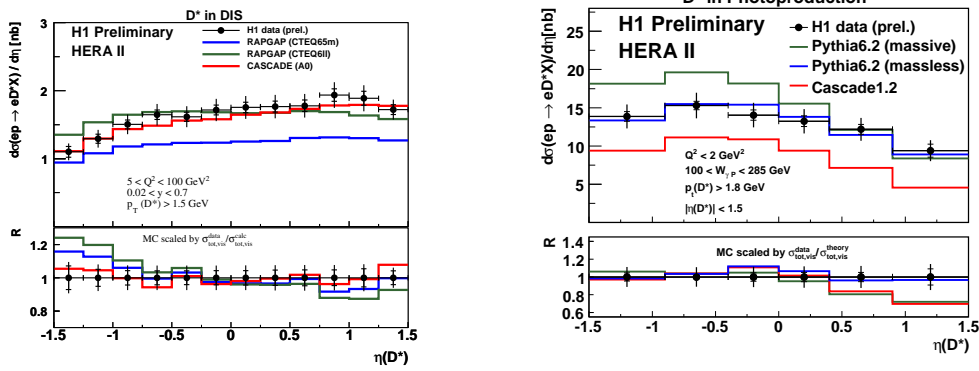


Figure 2: The $D^{*\pm}$ cross section as a function of $\eta(D^*)$ for the DIS (left) and photoproduction (right) regime.

double differential cross section measurement in y and Q^2 (DIS) a good agreement between the data and the NLO calculation HVQDIS is observed (see Figure 1 left). The increased y range down to 0.02 allows an additional bin in the double differential distribution which is well described by the NLO calculation. The $D^{*\pm}$ cross section as a function of $W_{\gamma P}$ in photoproduction as shown in Figure 1 (right) is neither described by the LO MC predictions nor by the NLO calculation to all details. The shape of the η distribution in DIS shown in Figure 2 (left) is described best with CASCADE. The Sensitivity to the proton PDF can

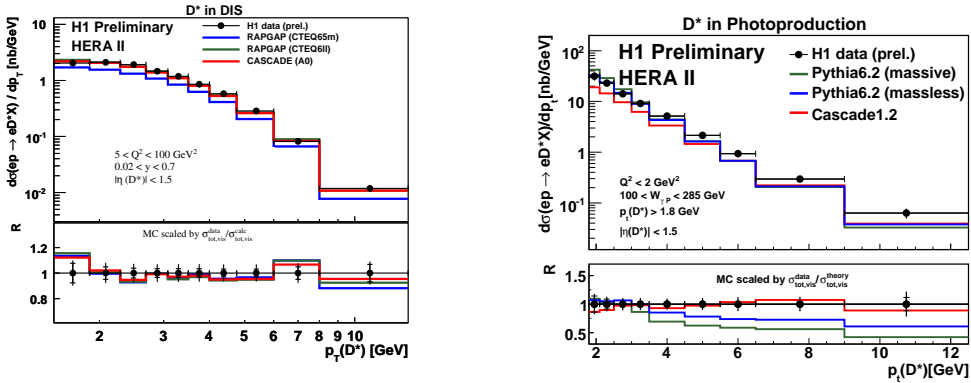


Figure 3: The $D^{*\pm}$ cross section as a function of p_T for the DIS (left) and photoproduction (right) measurement. The lower plots show the ratio.

be seen by the comparison to the RAPGAP MC which is shown with two proton PDFs: CTEQ61l [15] and CTEQ65m [16]. The normalised ratio at the bottom of the plot shows a better agreement to the data if the CTEQ65m PDF is used which uses a gluon density which provides a less steep rise towards small x . A small excess at forward directions $\eta > 0$ (seen previously in [7]) turns out to be located at low p_T as it can be seen in comparison to the NLO calculation for the double differential distribution (see Figure 4 left).

For the photoproduction regime, the η distribution shown at the right in Figure 2 shows a good description of the η shape by the massless PYTHIA calculation, which in contrast fails to describe the p_T shape as shown in Figure 3. At large p_T where the massless approach is expected to be appropriate the prediction is below the data. CASCADE describes the p_T shape but not the η shape at forward directions which might indicate missing contributions from resolved processes. In order to investigate the correlation between η and p_T the NLO calculation for the double differential distribution shown in Figure 4 is helpful; it turns out that neither the LO MC programs nor the NLO calculation (see Fig. 4 right) are able to describe the correlation between η and p_T in photoproduction. As shown in the right plot of Fig. 4 the NLO calculation shows an increasing deficit at forward $\eta > 0$ which is largest at high p_T -scale which allows reliable perturbative QCD calculations. Especially at high p_T basically all models including the LO MC predictions fail to describe the forward region and undershoot the data at $\eta > 0$.

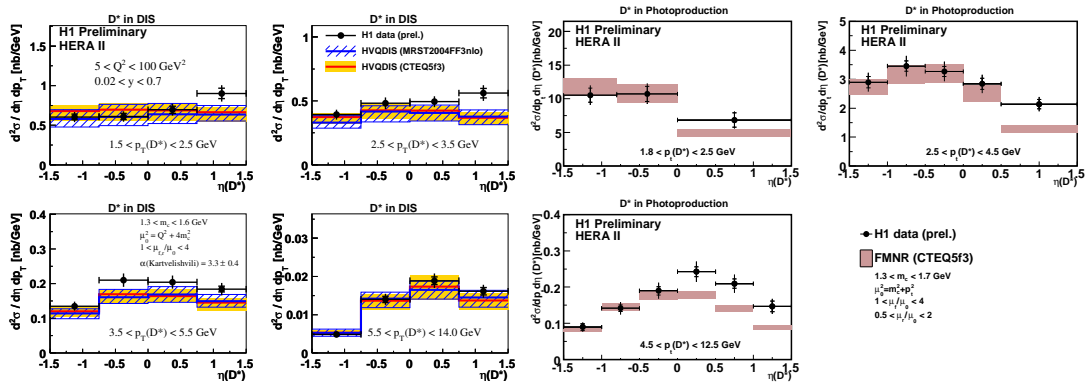


Figure 4: The double differential cross section in $\eta(D^*)$ and $p_T(D^*)$ for the DIS (left) and photoproduction (right) regime compared to the NLO calculation HVQDIS and FMNR.

5 Conclusions

Preliminary results from the H1 collaboration on inclusive $D^{*\pm}$ meson production in DIS and photoproduction have been presented. For the DIS sample overall a good description of the $D^{*\pm}$ data by the LO MC predictions and the NLO calculation is seen in single and double differential measurements. A small excess compared to the NLO calculation HVQDIS is seen at forward directions $\eta > 0$ which is located at low p_T . The shape of the η cross section is sensitive to different proton PDFs. The significance of the sensitivity is diminished by the relatively large theoretical uncertainties.

In the photoproduction regime data are less well described. Especially the $W_{\gamma P}$ dependence

is not described by the NLO calculation FMNR. The shape is reasonable described by the LO MC programs PYTHIA whereas CASCADE fails completely to describe the $W_{\gamma P}$ shape. The η shape is best described with PYTHIA (massless) which fails to describe the p_T shape, whereas CASCADE describes the p_T shape reasonably but fails for the η shape. In order to investigate the η - p_T correlation also double differential distributions have been measured. For the high p_T -region at forward $\eta > 0$ all MC models and the NLO-calculation FMNR fail to describe the data although a large scale is provided by p_T .

References

- [1] <http://indico.cern.ch/contributionDisplay.py?contribId=238&sessionId=14confId=24657>.
- [2] A. Aktas et al. *Eur. Phys. J.C*, **50**:251, 2006.
- [3] A. Baird et al. *IEEE Trans. Nucl. Sci.*, **48**:1276, 2001.
- [4] A. Schöning. *Nucl. Instr. and Meth.*, **A518**:542, 2004.
- [5] A.W. Jung et al. "First Results from the Third Level of the H1 Fast Track Trigger". *Proc. of the 2007 IEEE NPSS RealTime Conference*, 2007.
- [6] U. Bassler, G. Bernardi. *Nucl. Instr. and Meth.*, **A361**:197, 1995.
- [7] A. Aktas et al. *Eur. Phys. J.C*, **51**:271, 2007.
- [8] Sjöstrand, et al. *Comput. Phys. Commun.*, **135**:238, 2001.
- [9] H. Jung,. *Comput. Phys. Commun.*, **143**:100, 2002.
- [10] S. Frixione, M.L. Mangano, P. Nason and G. Ridolfi. *Phys. Lett. B*, **384**:633, 1995.
- [11] B. W. Harris and J. Smith. *Nucl. Phys. B*, **452**:109, 1995.
- [12] H. L. Lai, et al. *Eur. Phys. J.C*, **12**:375, 2000.
- [13] A.D. Martin, W.J. Stirling, R.S. Thorne. *Physics Letters B*, **636**:259, 2006.
- [14] H. Jung,. *Comput. Phys. Commun.*, **86**:147, 1995.
- [15] J. Pumplin, et al. *JHEP*, **012**:07, 2002.
- [16] W.K. Tung, et al. *JHEP*, **0702**:053, 2007.